JYX
JYVÄSKYLÄN YLIOPISTO
UNIVERSITY OF JYVÄSKYLÄ

This is a self-archived version of an original article. This version may differ from the original in pagination and typographic details.

Author(s): Toivanen, V.; Bhaskar, B. S.; Izotov, I. V.; Koivisto, H.; Tarvainen, O.

Title: Diagnostic techniques of minimum-B ECR ion source plasma instabilities

Year: 2022

Version: Published version

Copyright: © 2022 Author(s).

Rights: In Copyright

Rights url: http://rightsstatements.org/page/InC/1.0/?language=en

Please cite the original version:

Toivanen, V., Bhaskar, B. S., Izotov, I. V., Koivisto, H., & Tarvainen, O. (2022). Diagnostic techniques of minimum-B ECR ion source plasma instabilities. Review of Scientific Instruments, 93(1), Article 013302. https://doi.org/10.1063/5.0075443

Review of Scientific Instruments

Diagnostic techniques of minimum-B ECR ion source plasma instabilities

Cite as: Rev. Sci. Instrum. **93**, 013302 (2022); https://doi.org/10.1063/5.0075443
Submitted: 15 October 2021 • Accepted: 17 December 2021 • Published Online: 04 January 2022

V. Toivanen, B. S. Bhaskar, I. V. Izotov, et al.

COLLECTIONS

Paper published as part of the special topic on Ion Source Diagnostics

View Online Export Citation CrossMark

ARTICLES YOU MAY BE INTERESTED IN

Ultrafast time- and angle-resolved photoemission spectroscopy with widely tunable probe photon energy of 5.3–7.0#eV for investigating dynamics of three-dimensional materials
Review of Scientific Instruments **93**, 013902 (2022); https://doi.org/10.1063/5.0070004

Posture adjustment and robust microinjection of zebrafish larval heart
Review of Scientific Instruments **93**, 014101 (2022); https://doi.org/10.1063/5.0064563

Compact, tunable polarization transforming reflector for quasi-optical devices used in terahertz science
Review of Scientific Instruments **93**, 013102 (2022); https://doi.org/10.1063/5.0036292

AMSTERDAM SCIENTIFIC INSTRUMENTS
www.amscins.com
3D IMAGING of Ions & Electrons
Perfect replacement for conventional 2D cameras
TPX3CAM READOUT
TIME OF FLIGHT EXPERIMENT 29.05.2021

ToA (sec)	ToT (nanosec)	Coordinates	
Time of Arrival	Time over Threshold	X	Y
1.134267353184	425	144	140
1.134267353162	875	57	234
1.134267353137	875	235	149
1.134267353120	125	178	140
1.134267353111	975	5	130

AIP Publishing

© 2022 Author(s).

Review of Scientific Instruments ARTICLE scitation.org/journal/rsi

Diagnostic techniques of minimum-B ECR ion source plasma instabilities

Cite as: Rev. Sci. Instrum. 93, 013302 (2022); doi: 10.1063/5.0075443
Submitted: 15 October 2021 • Accepted: 17 December 2021 •
Published Online: 4 January 2022

View Online Export Citation CrossMark

V. Toivanen,[1,a)] B. S. Bhaskar,[1,2] I. V. Izotov,[3] H. Koivisto,[1] and O. Tarvainen[4]

AFFILIATIONS

[1] Department of Physics, University of Jyväskylä (JYFL), 40500 Jyväskylä, Finland
[2] Univ. Grenoble Alpes, CNRS, Grenoble INP, LPSC-IN2P3, 38000 Grenoble, France
[3] Institute of Applied Physics of Russian Academy of Sciences, 603950 Nizhny Novgorod, Russia
[4] STFC ISIS Pulsed Spallation Neutron and Muon Facility, Rutherford Appleton Laboratory, Harwell OX11 0QX, United Kingdom

Note: This paper is a part of the Special Topic Collection on Ion Source Diagnostics.
[a)] **Author to whom correspondence should be addressed:** ville.a.toivanen@jyu.fi

ABSTRACT

The performance of a minimum-B Electron Cyclotron Resonance Ion Source (ECRIS) is traditionally quantified by measuring the beam current and quality of the extracted ion beams of different charge state ions. The stability of the extracted ion beam currents has drawn more attention recently as the technology is pushing its limits toward higher ion charge states and beam intensities. The stability of the extracted beam is often compromised by plasma instabilities manifesting themselves as rapid oscillations of the beam currents in millisecond scale. This paper focuses on practical aspects of diagnostics techniques of the instabilities, showcases examples of instability-related diagnostics signals, and links them to the plasma physics of ECR ion sources. The reviewed techniques include time-resolved microwave emission diagnostics, bremsstrahlung measurements, direct measurement of electron and ion fluxes, measurement of the ion beam energy spread, and optical emission diagnostics. We list the advantages and disadvantages of each technique and outline the development needs of further diagnostics. Finally, we discuss the implications of the instabilities in both historical and forward-looking context of ECRIS development.

Published under an exclusive license by AIP Publishing. https://doi.org/10.1063/5.0075443

I. INTRODUCTION

Electron cyclotron resonance ion sources (ECRIS)[1] are widely used in accelerator facilities for the production of intense beams of highly charged heavy ions. The magnetic field of a modern ECRIS is a superposition of solenoid and sextupole fields. The resulting minimum-B topology provides a closed surface for resonant energy transfer from microwaves to the plasma electrons, enables sufficient plasma confinement for the ionization of high charge states, and suppresses magnetohydrodynamic instabilities.[2] ECRIS plasmas are strongly anisotropic and are considered to consist of cold electrons with an average energy $E_{e,\,cold}$ of 10–100 eV, warm electrons responsible for the ionization with $E_{e,\,warm}$ of 1–10 keV, and hot electrons with $E_{e,\,hot}$ of 10–100 keV.[3,4] Such non-equilibrium plasmas are prone to kinetic maser-type instabilities[5,6] driven by hot electrons whose transverse velocity ($v \perp B$) dominates over the longitudinal one ($v \parallel B$).

The instabilities lead to oscillation of the extracted beam current in ms-scale (see, e.g., Ref. 7) and the beam energy in μs-scale.[8,9] Such oscillations, restricting the parameter space available for optimization of the source performance, are often overlooked by the ion source operator attempting to single-mindedly maximize the average beam current with limited diagnostics. An illustrative example of the instability-induced periodic oscillations of the extracted beam current and the corresponding Fourier spectrum is shown in Fig. 1. Fast fluctuations of beam current and energy are especially problematic for modern applications of ECR ion sources requiring supreme temporal stability, e.g., hadron therapy[10] and material modification,[11] high power accelerators due to increased beam spill at high beam energy, and charge breeding applications where the instabilities increase the level of unwanted contaminants in the beam current.[12]

The kinetic instabilities found in minimum-B devices have a distinct fingerprint as they lead to bursts of microwave emission

Published under an exclusive license by AIP Publishing

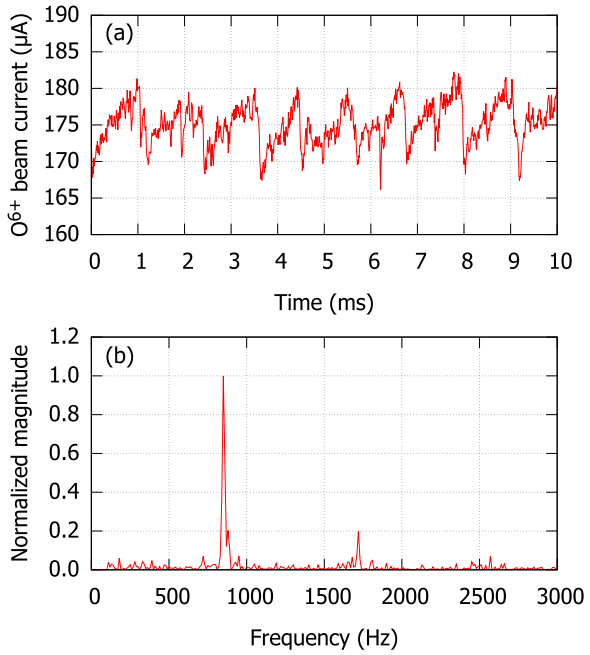

FIG. 1. An example of instability-induced oscillation of O^{6+} beam current (a) and the corresponding frequency spectrum which highlights the periodic nature of the current variation (b). Measured with the JYFL 14 GHz ECRIS.

at frequencies close to the plasma heating frequency and abrupt particle (electron and ion) losses from the trap. The description of the physical phenomena triggering the instabilities and determining their growth and damping rates as well as energy and particle losses can be found from the literature (see, e.g., Refs. 13 and 14). In short, the instability sequence proceeds as follows; once the energy content and anisotropy of the electron energy distribution (EED) exceeds a threshold where the instability growth rate $\gamma \propto \frac{N_{e,hot}}{N_{e,cold}}$ overcomes the instability damping rate δ, electrons interacting with the amplifying plasma wave emit microwave radiation and are expelled into the loss cone of the magnetic confinement. The increased flux of electrons from the trap leads to an abrupt burst of wall bremsstrahlung and relaxation of the EED into a stable one. The ions, which have lower mobility than the electrons, are first left behind causing the ambipolar potential to increase momentarily before a burst of ions restores the quasi-neutrality. The sequence repeats quasi-periodically as the plasma recovers from the instability onsets. The recovery is best seen in the beam currents of high charge state ions exhibiting periodic oscillation.

The resulting signals indicating the presence of kinetic instabilities can be observed with non-invasive time-resolved diagnostics methods, e.g., microwave and bremstrahlung detectors. Such diagnostics have been first developed for experiments of simple mirror confinement for thermonuclear fusion with minimum-B devices.[15,16] For minimum-B ECRIS, they can be used for monitoring the transition between stable and unstable plasma regimes (typically with varying B-field strength) and for obtaining information on the ECRIS plasma properties and their parametric dependencies.

In the following sections, we review the diagnostics techniques of kinetic instabilities in ECRIS plasmas and present highlights of experimental results obtained through each diagnostics method. Furthermore, we outline the needs for further development of instability diagnostics and discuss potential experiments that could follow.

II. MICROWAVE EMISSION

Microwave emission is the primary diagnostics signal related to the kinetic instabilities of mirror-confined minimum-B ECR-heated plasmas.[15] Microwave emission diagnostics are complicated by mechanical constraints of the ECRIS plasma chamber, prohibiting access for a wideband microwave receiver. Thus, the detection of instability-induced microwave bursts often relies on using secondary waveguide ports found in the vast majority of ion sources operating at frequencies ≥10 GHz, i.e., the microwave signal is affected by the coupling efficiency into the "diagnostics waveguide,"

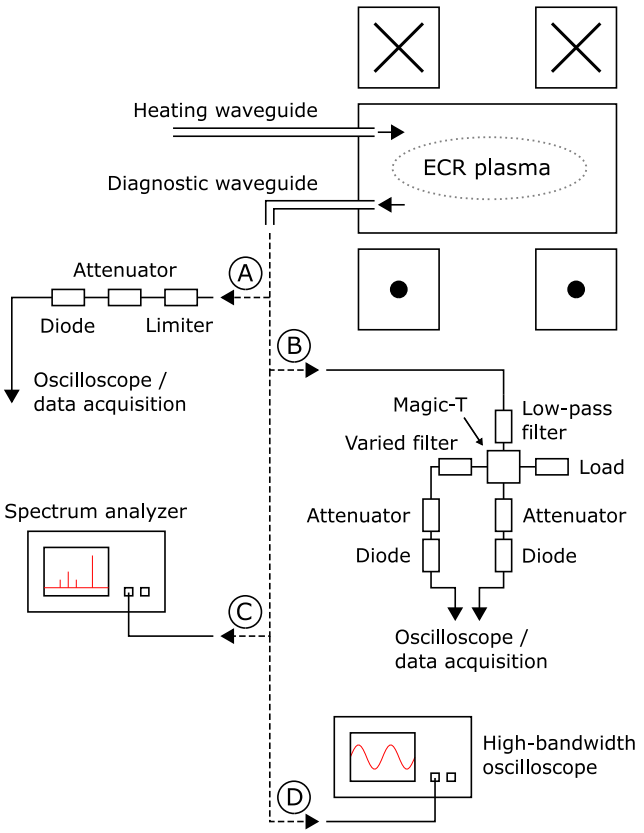

FIG. 2. Schematic example setups for the different microwave diagnostic techniques connected to the secondary waveguide of an ECRIS. The examples include (A) a simple measurement with a Schottky diode, (B) a more complex setup using a Magic-T and different waveguide filters to acquire additional frequency information (following the presentation in Ref. 25), (C) a spectrum analyzer, and (D) a high-bandwidth oscilloscope. Instead of using a waveguide connection, spectrum analyzers and oscilloscopes can directly measure the free space emission from the ion source with a suitable broadband antenna (not shown in the figure).

Published under an exclusive license by AIP Publishing

the (frequency-dependent) attenuation by the waveguide transmission, and the efficiency of the microwave detection system itself. Nevertheless, several diagnostics techniques have been employed to detect the instability-induced microwaves and measure the emission frequencies from minimum-B ECRIS plasmas. They include microwave-sensitive low barrier Schottky diodes,[7,12,17–19] spectrum analyzers,[20] and high-bandwidth oscilloscopes.[21–24] The schematics of each detection setup is presented in Fig. 2.

The simplest technique to detect instability-induced microwave emission bursts (an example is shown in Fig. 3) is to connect a low barrier Schottky diode to the secondary waveguide port. The diodes are sensitive to microwave radiation in the wide frequency range, e.g., 0.01–50 GHz in Ref. 7, which means that the detection bandwidth is often limited by the waveguide (e.g., WR-75 with 7.9 GHz cutoff) and auxiliary components such as limiters, attenuators, and connectors (typically limited to frequencies below 26.5 GHz). Limiters and attenuators are not strictly necessary but since the microwave emission power coupled into the waveguide during the instability burst can easily exceed several kW (especially in the afterglow mode), these components are needed to protect the diode. Furthermore, the microwave transfer line can be equipped with a magic-T component, which allows using the waveguide simultaneously for secondary frequency heating and detection of the plasma emission.[24] The benefit of the Schottky diode is the ease of operation as its output can be connected directly to an oscilloscope and/or data acquisition system, and the <10 ns temporal resolution. The obvious drawback of the diode is the lack of information on the plasma emission frequencies. Orpana *et al.*[25] demonstrated a low-cost technique, based on Schottky diodes, to approximate the microwave emission frequencies induced by plasma instabilities. In their experiments, the microwave signal was split between two waveguide branches with a magic-T with one of the branches equipped with high-pass waveguide filter(s). The emission signals were then detected with Schottky diodes terminating each waveguide branch, and the two signals, obtained with various filters, were compared to approximate the emission frequencies.

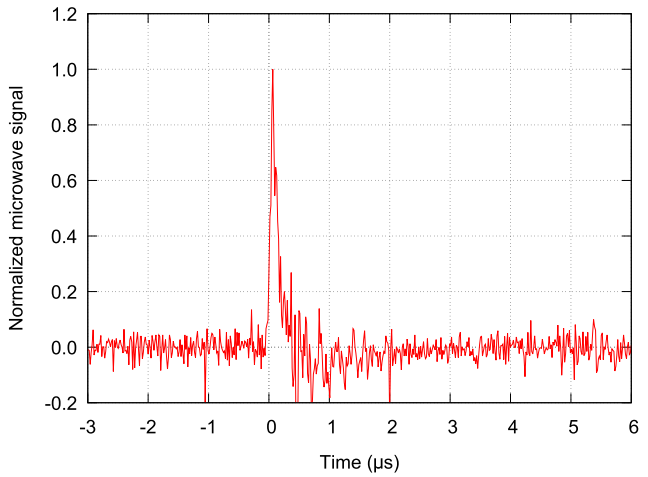

FIG. 3. An example of instability-induced microwave signal measured with a Schottky diode connected to the diagnostic waveguide of JYFL 14 GHz ECRIS.

The frequencies of the instability-induced microwave emission can be detected with a spectrum analyzer connected at the end of the diagnostics waveguide, to an RF-probe protruding into the plasma chamber, or to an external receiver placed in the proximity of the ion source radiating into free space. Each method requires different degrees of protection for the spectrum analyzer as the signal level depends strongly on the coupling from the ion source plasma into the spectrum analyzer input via the receiver. Naselli *et al.*[20] described experiments on a minimum-B ECRIS using a double-pin RF probe protruding into the plasma chamber through a gas feed aperture. The experiments in Ref. 20 confirmed that the emission frequencies are typically lower than the plasma heating frequency and that the energy dissipated via microwave emission increases with the plasma energy content controlled by the ion source parameters such as microwave heating power. The drawback of the spectrum analyzer technique is the lack of temporal information on the microwave emission and the possibility of discounting emission frequencies. This is because the analyzer sweeps across a range of frequencies (divided into a discrete number of channels) and records the signal at each frequency step over a certain dwell time, which depends on the sweep time selected by the user. Examples of emission spectra recorded with a spectrum analyzer are shown in Fig. 4 for varying sweep times. The given example serves to demonstrate that at fast sweep times, only continuous or most prevalent instability emission frequencies are detected, while at sufficiently long sweep times, the

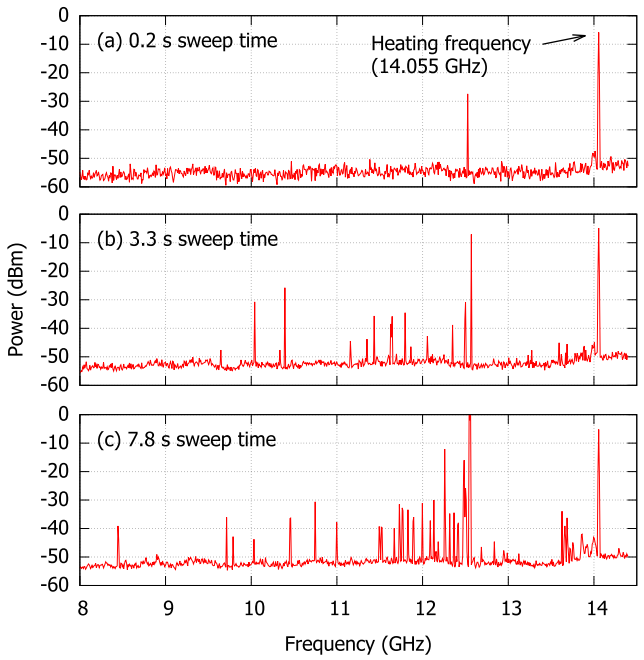

FIG. 4. An example of the spectrum analyzer signal (power spectrum) measured with a Keysight FieldFox Microwave Analyzer N9918B[27] using three different frequency sweep times: (a) 0.2 s, (b) 3.3 s, and (c) 7.8 s. The measurement was performed outside the ion source with an external antenna during unstable plasma conditions. The continuous plasma heating frequency (14.055 GHz) is indicated with an arrow. The other peaks are associated with the instability-induced microwave emissions. The data were measured with the JYFL 14 GHz ECRIS.

Published under an exclusive license by AIP Publishing

spectrum becomes richer revealing weaker emission signals. Spectrum analyzers are available up to 110 GHz frequency,[26] i.e., there are no apparent technological limitations preventing the described technique to be used for high-frequency third and fourth generation minimum-B ECR ion sources.

The preferred method of detecting the instability-induced microwave emission is to measure the microwave radiation electric field directly with a high-bandwidth oscilloscope connected to the diagnostics waveguide port or measuring the free space emission with a broadband short dipole antenna.[23] Direct measurement of the microwave electric field enables detecting the emission frequencies and their temporal variation in sub-nanosecond time scale as demonstrated in Fig. 5, showing an example of the instability-induced microwave emission measured with a high-bandwidth oscilloscope. Utilizing an oscilloscope is superior to the diode and spectrum analyzer in terms of acquired information but requires rather extensive post-processing of the data, e.g., converting the raw oscilloscope data into spectral power density plots revealing the temporal evolution of the microwave emission power and frequency as shown in Fig. 5. Another benefit of the oscilloscope technique is that the measurement can be easily triggered, e.g., by the plasma heating microwave pulse, which allows measurements to be taken in continuous as well as in the afterglow (pulsed) operation mode of the ion source as described in Ref. 28. The method requires the bandwidth of the oscilloscope to exceed the microwave emission frequency. In practice, this means that detection of all harmonics of the emission requires the oscilloscope bandwidth to be >2 times the main heating frequency. The development of oscilloscopes has been recently driven by the emergence of 5G data transfer technology, and similar to the spectrum analyzers, the bandwidth of state-of-the-art oscilloscopes extends up to 110 GHz.[29] As such, modern oscilloscopes cover the expected range of microwave emission frequencies of next generation minimum-B ECR ion sources operating at very high frequencies.[30]

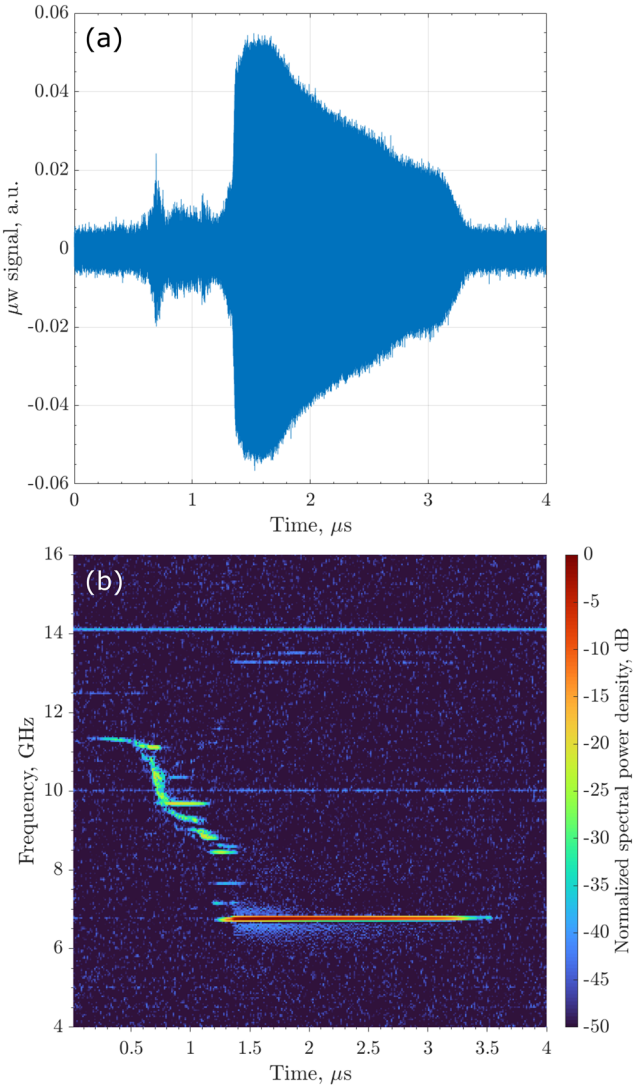

FIG. 5. An example of instability-induced microwave emission measured with a high-bandwidth oscilloscope. The measured raw waveform is presented in (a) and the corresponding post-processed spectrogram in (b). The data were measured with the JYFL 14 GHz ECRIS.

The vast majority of microwave emission measurements on minimum-B ECR ion sources have been carried out with second generation devices operating at 14 GHz plasma heating frequency. The main findings of these experiments can be summarized as follows: (1) The microwave emission burst typically lasts for 10–100 ns (order of magnitude).[22] (2) The emission frequencies are concentrated below the main plasma heating frequency with harmonics observed at higher frequencies.[22,23] (3) The emission frequencies are discrete and often independent on the ion source parameters.[22] (4) The microwave emission related to an instability-event often consists of several consecutive chirps separated by 1–10 μs (order of magnitude).[22,31] (5) The emission frequencies within these chirps and those of the consecutive chirps have a falling tone, which implies the excitation of the quasi-longitudinal Z-mode.[31] (6) The microwave emission power of afterglow instabilities is stronger than the emission power associated with onsets of periodic instabilities in the continuous plasma heating mode.[22,31]

III. ELECTRON FLUX

Following the sequence of events in the instability process, the second observable is the sudden flux of electrons that are expelled from the plasma as a result of the energy transfer to the plasma wave and the consequent loss of confinement. In principle, the electron losses can be measured directly inside the plasma chamber with a dedicated probe, which is typically hampered by the mechanical constraints of the ion source design. Another alternative is to measure the electron flux that escapes the plasma chamber through the extraction aperture. Both of these approaches are discussed in the following text.

The majority of modern ECR ion sources are equipped with a biased disk at the injection end of the plasma chamber, at the location where the flux of lost electrons (and ions) intercepts the axial wall of the chamber. During an instability event, a burst of lost electrons (followed by ions) impinge on the biased disk, causing a fast current transient in the disk circuit. Monitoring the

Published under an exclusive license by AIP Publishing

biased disk current for these transients can be used as a diagnostic method to determine the presence of plasma instabilities, as has been reported by Isherwood *et al.*[19] Furthermore, the disk can be used as a rudimentary Langmuir probe to quantify these instability-induced electron (and ion) losses, as has been demonstrated by Tarvainen *et al.*[9] The instability-induced fast current transients can reach up to hundreds of milliamperes in a sub-μs time scales. The power supplies that are typically used with biased discs are not able to handle this kind of sudden current surges. In order to overcome the issue and to ensure adequate temporal resolution for the current measurement, the circuit between the biased disk and the power supply needs to be amended with an additional capacitor placed in parallel with the power supply to act as a charge storage. The current signal flowing in the circuit can be monitored by measuring the voltage across a resistor placed in series with the biased disk. A schematic example of the measurement circuit is presented in Fig. 6.

An example of a typical instability-induced current signal measured from the biased disk is presented in Fig. 7. The initial negative current transient is produced by the burst of axially lost electrons. The electron losses create a significant increase in the ambipolar potential of the plasma, resulting in an ion current transient (positive), which restores the plasma quasineutrality. The electron and the ion transients carry approximately an equal amount of total charge, i.e., the areas of the negative and positive transient peaks are approximately the same.[9] The combined duration of the electron and ion transients is typically less than 10 μs, with the ion transient being the longer one due to the lower mobility of ions. During the instability-induced sequence, the measured transient currents can be 1–2 orders of magnitude higher than the steady state current of the biased disk.

Several methods to measure the electron flux that escapes the ion source plasma chamber during the instabilities have been demonstrated over the years, concentrating on detecting the electrons that escape the confinement axially through the extraction aperture. Perhaps the simplest method is to use a suitable semiconductor detector placed on the source axis inside the extraction

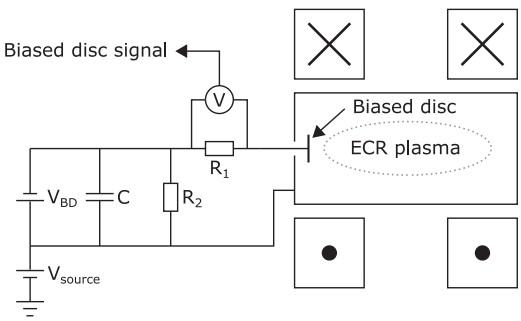

FIG. 6. A schematic example of a circuit to measure the instability-induced current transients from the biased disk of an ECR ion source. V_{BD} is the voltage provided by the biased disk power supply with respect to the source potential V_{source}, R_1 is the resistor to monitor the biased disk current, capacitor C acts as a charge storage to enable measurements of fast current transients, and R_2 is the capacitor discharge resistor. It is noted that the measured signal is on the source HV and, thus, requires electrical decoupling (e.g., with an optical isolator) if the data acquisition is placed outside the ion source HV enclosure.

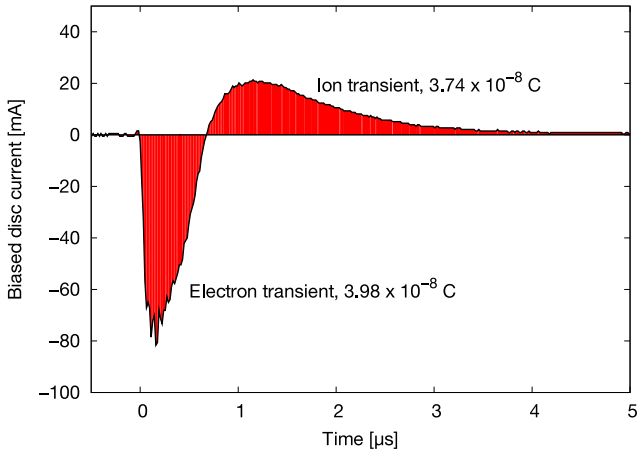

FIG. 7. An example of a typical instability-induced current signal measured from the biased disk of JYFL 14 GHz ECRIS. The signal comprises of the initial electron burst (negative signal) followed by the ion contribution (positive signal). Reproduced from Tarvainen *et al.*, Rev. Sci. Instrum. **90**, 123303 (2019) with the permission of AIP Publishing.

vacuum vessel or a diagnostic chamber to directly measure the escaping electron flux. For example, Refs. 32–36 describe a series of studies that use a PIN diode to investigate the instability-induced electron precipitations from axisymmetric mirror magnetic trap that occur during the decay phase of a pulsed ECR discharge. The electron detection with a PIN diode is based on the production of charge carriers in the intrinsic semiconductor region of the diode by the impinging electrons. This generates a current pulse in the circuit with an amplitude which is proportional to the deposited electron energy. The diode structure sets the lower and upper limits for the energy of electrons that can be detected. The lower limit is defined by the thickness of the dead layer in the diode, whereas the upper limit is set by the size of the depleted zone in the intrinsic region. The drift time of the charge carriers across the sensitive region determines the diode time resolution. As an example, the PIN diode used in the experiments described in Ref. 32 (type SPPD-11-04) can detect electrons with energies between 7 and 500 keV with a time resolution of a few nanoseconds, which makes it well suited for studies of the escaping hot electrons during the instability events. Diodes are also sensitive to x-ray photons, so precautions are necessary to ensure that x-ray emissions from the plasma do not influence the electron measurements.

The main limitation of using a simple diode diagnostic is the lack of electron energy information. This can be amended by introducing a separate filtering system in front of the diode to sample the energies of the escaping electrons. A filtering system comprising a set of movable Al foils of different thicknesses in front of a PIN diode has been presented in Ref. 32. The thickness of the used foil determines a low energy cutoff for the measured electron flux. a set of foils with known thicknesses and the corresponding cutoff electron energies can be used to determine the energy distribution of the escaping electrons with discrete steps. This method has been developed further in Ref. 37 where the PIN diode was replaced with a Faraday cup. This removes the lower and upper energy limitations

Published under an exclusive license by AIP Publishing

of the diode from the measurement as well as the issue of the electron measurement being sensitive to x-ray photons.

Energy dispersive separators (spectrometers) can be used downstream from the ion source to acquire more comprehensive information about the energy distribution of the axially escaping electrons. In Ref. 38, Izotov *et al.* demonstrated the direct measurement of the energy distribution of axially escaping electrons from a stable ECR plasma using the ion source spectrometer magnet—originally designed for the m/q separation of multiply charged ions—as an electron energy analyzer. The technique has been used also in other studies for investigations of both stable and unstable ECR plasmas[39,40] in the time-averaged mode, i.e., by measuring the average electron current for each electron energy step. As plasma instabilities are characterized by the abrupt current transients, this time-averaged method provides only limited information of the expelled electrons. In Refs. 41 and 42, Izotov *et al.* demonstrated the use of the method in the time-resolved mode to determine the temporal evolution of the measured electron energy distribution, making it the state-of-the-art diagnostic technique for studies of instability-induced axial electron losses from ECRIS plasmas.

In order to measure the electron energy distribution, the polarity of the ion source spectrometer magnet is reversed from the normal operation condition intended for positive ions. Usually, this requires replacement of the original power supply with the one that has higher precision and a suitably small current step to provide sufficient sampling of the electron energy. The maximum current of the power supply also defines the maximum measurable electron energy. A calibrated Hall-probe can be used to accurately determine the magnetic field inside the magnet to allow precise calculation of the corresponding electron energy. The energy distribution of the electrons escaping from the source is then determined by ramping the magnetic field of the spectrometer and measuring the electron current downstream from the magnet. In time-sampled measurement of plasma instabilities, the time evolution (waveform) of the electron current is measured for each energy bin of the electron energy distribution, i.e., each spectrometer B field step. To synchronize the data acquisition, each waveform should be triggered by an instability event. A secondary instability diagnostic can be used to provide this signal, for example, in Ref. 41, the microwave emission measured with a diode was used to trigger the electron measurement. Finally, all the waveforms can be combined to show the temporal evolution of the energy distribution. An example is presented in Fig. 8.

Several options exist for the electron detector. Isherwood and Machicoane[39] demonstrated the use of a precise current monitoring with a Faraday cup for this purpose, whereas the system used by Izotov *et al.*[38,41] uses a secondary electron amplifier to measure the electron current. With this method, secondary electrons are emitted from a biased cathode, which are then multiplied by a chain of subsequent grid stages. The final amplified current is read from the grounded anode with a picoammeter or a transimpedance amplifier. It is noted that the cathode bias voltage sets a lower limit for detectable electron energies. For example, in Ref. 38, −4 kV cathode voltage was used, which sets a lower limit of 4 keV for measured electron energies. In order to determine the energy resolution for the measurement, the electron flux from the ion source is limited with a set of grounded collimators which are placed between the source

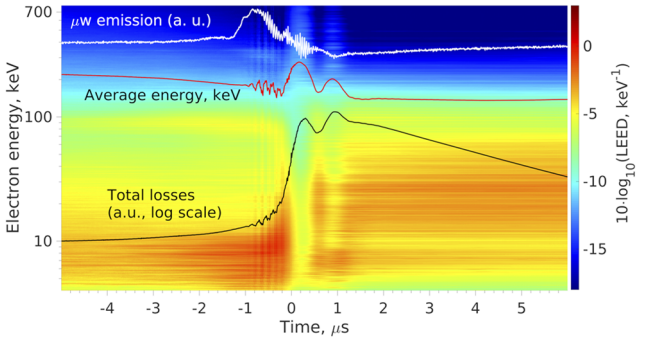

FIG. 8. An example of axially lost electron energy distribution as a function of time during a plasma instability event. The calculated total electron flux, average electron energy, and the simultaneously measured microwave signal are also shown. Reproduced from Izotov *et al.*, Rev. Sci. Instrum. **91**, 013502 (2020) with the permission of AIP Publishing.

and the detector. As an example, the setup presented in Refs. 38 and 41 used three collimators with 5 mm diameter apertures, which provided an estimated energy resolution below 500 eV. A schematic example of the measurement setup is presented in Fig. 9.

Several correction factors need to be taken into account during the data analysis to obtain the correct shape of the escaping electron energy distribution. First, the transmission efficiency of electrons from the source to the detector is energy dependent. A correction function can be determined for this with ion optical simulations of the electron transport through the beamline and the spectrometer magnet, taking into account the electron collimation scheme used in the measurements. In addition, all focusing electrodes along the electron path should be carefully grounded and all magnetic elements (solenoids, steering magnets, etc.) switched off to avoid influencing the electron trajectories and thereby affecting their energy dependent transmission efficiency. Second, if the electron current is measured with a secondary electron amplifier, the

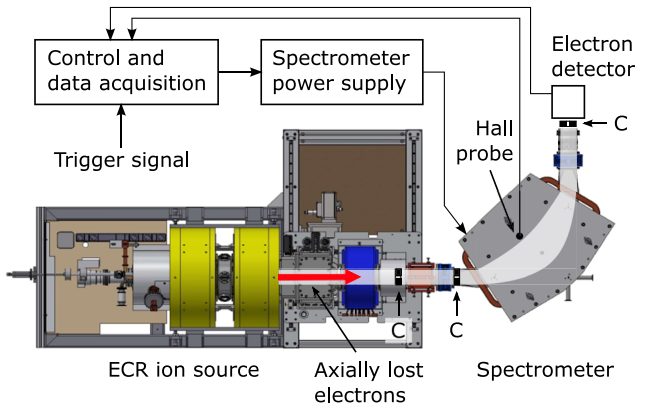

FIG. 9. A schematic example of a setup to measure the axially lost electron energy distribution with the ion source spectrometer magnet. The example includes three electron collimators along the beamline indicated with *C*. The time-sampled measurement requires a trigger signal from the onset of the instability to synchronize the data acquisition.

Published under an exclusive license by AIP Publishing

energy dependent yield of the secondary electrons from the detector cathode as well as the electron back scattering should be taken into account.

The main findings from the electron flux studies related to plasma instabilities can be summarized as follows: (1) The typical time scale for the duration of an individual instability-induced electron burst is 0.1–1 μs (order of magnitude), and usually, several consecutive bursts are observed following the onset of the instabilities.[34,37] (2) Estimations based on the results of the biased disk studies imply that the fraction of electrons expelled during each instability burst can be on the order of 10% of the total electron population.[9] (3) The instabilities cause electron losses across the whole range of the electron energy distribution (see, e.g., Refs. 9 and 41). (4) Compared to the situation preceding the onset of instabilities, the energy distribution of the escaping electrons changes drastically during the instability event with enhanced losses of high energy electrons and a consequent increase in the average escaping electron energy (see Fig. 8).[41]

IV. BREMSSTRAHLUNG

As illustrated above, the instability process induces a sudden loss of high-energy plasma electrons. The duration of the electron burst is on the order of a microsecond, and its power flux can exceed the background level of continuous electron losses by several orders of magnitude. The lost electrons follow the magnetic field lines and they can escape from the plasma chamber through the extraction aperture (as discussed in Sec. III) or they can interact with the plasma chamber structures at the magnetic poles generating thick target bremsstrahlung in this interaction point. The instability-induced bremsstrahlung transient and its properties, such as amplitude, power, repetition rate, and energy spectrum, can be studied to obtain information about the plasma parameters, triggering the plasma instabilities and affecting the plasma processes during the instability event.

The instability-induced radiation transient and its properties can be studied using conventional x-ray diagnostics such as (a) x-ray scintillators coupled with photomultiplier tubes (PMT) or (b) energy sensitive semiconductor detectors. In both cases, the attenuation and scattering of photons in the surrounding structures has to be minimized to avoid, for example, the distortion of the measured bremsstrahlung spectrum and the signal amplitude. In addition, proper shielding of the detector and all relevant calibrations and corrections need to be made to minimize the uncertainties. The afore-mentioned diagnostic methods to study instability-induced bremsstrahlung transients will be discussed hereafter.

A. Scintillator and photomultiplier tube

Scintillators have a wide variety of applications, but in the context of this article, we focus on their application to detecting fast changes in the power flux of bremsstrahlung radiation associated with kinetic plasma instabilities. The instability-induced bremsstrahlung photon is absorbed by the scintillator material causing electron excitations when interacting with the material. The volume and material of the scintillator are important factors as they are strongly linked to the detection efficiency, especially for the high-energy tail of the bremsstrahlung spectrum. As a result of the x-ray photon absorption and the subsequent de-excitations, the material emits a pulse of photons typically in the visible light spectrum (300–800 nm). The scintillator material is highly transparent to its own fluorescence emission, and therefore, the emitted photon pulse can be detected outside the scintillator.

The emitted photon pulse from the scintillator is typically detected either with a photocathode followed by a photomultiplier tube (PMT) or with a photodiode to convert the photon flux to a current of electrons. The magnetic field strongly affects the operation of PMTs, and consequently, a proper shielding has to be applied to suppress the stray field of the ion source. The vast majority of plasma instability experiments have used PMTs, and consequently, this setup is presented here in further detail.

Figure 10 is a schematic showing the operating principle and the main elements of the scintillator + PMT setup: (1) scintillator, (2) photocathode, (3) photomultiplier tube (dynodes and collector anode), and (4) signal processing unit. The scintillator absorbs the incoming radiation and converts it to visible light. The scintillation light interacts with the light-sensitive low work-function photocathode, which converts the photon signal to a current of electrons via the photoelectric effect. The spectral efficiency of the photocathode is energy dependent and depends on the choice of the photocathode material. The electron current from the photocathode is then amplified by a chain of dynode electrodes. The electron current is amplified by each dynode via the process of secondary electron emission, increasing the electron current exponentially, and resulting in a measurable signal at the collector (anode), at the end of the photomultiplier tube. The total gain of the PMT depends on the number of dynodes and on the bias voltage applied across the amplification chain. The magnetic field shielding must be designed to minimize the field component transverse to the dynode chain, potentially deflecting the electrons.

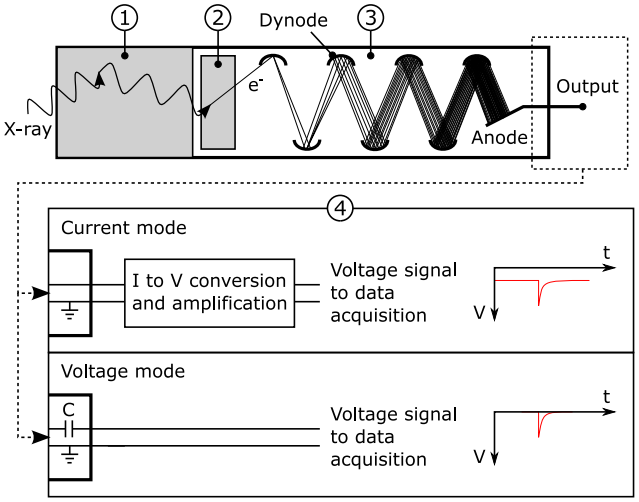

FIG. 10. A schematic of an x-ray scintillator coupled with a photomultiplier tube and the connection to a data acquisition system for operation in current (DC) and voltage (AC) modes. The system consists of (1) x-ray scintillator, (2) photocathode, (3) photomultiplier tube, and (4) output signal processing for current and voltage mode PMT operation.

Published under an exclusive license by AIP Publishing

The photomultiplier tube can be operated either in the current (DC) or voltage (AC) mode, as shown in Fig. 10. In the current mode, the PMT anode is connected directly to a transimpedance amplifier further amplifying and converting the output signal to a voltage, which is then recorded with an oscilloscope or any other data acquisition system. In this mode, the continuous background radiation is measured and the fast transient induced by the instability event is seen as an abrupt signal peak above the background level (see Fig. 11 as an example). The signal amplitude is proportional to the power flux of the incident radiation. In the voltage mode, the PMT output is measured across a capacitor connected between the anode and the signal output. In this configuration, only fast changes of the x-ray power flux are measured. The output voltage is proportional to $d\Phi/dt$, where Φ is the incoming x-ray power flux, and the signal can be connected directly to the input impedance of an oscilloscope (keeping in mind the effect of the circuits RC-constant on the temporal resolution). More information about the operating methods of photomultiplier tubes can be found, for example, from Ref. 43.

The majority of the ECRIS plasma instability-related bremsstrahlung measurements have been performed using bismuth germanate (BGO) scintillators because their properties are sufficient for the instability diagnostics and they are often readily available in many accelerator laboratories. General properties of the BGO-material, e.g., the energy range, can be found from Ref. 44. The fluorescence decay time of the BGO is about 300 ns and the typical time characteristic of PMTs is less than 100 ns, which makes the system well suited for measurements of fast instability-induced x-ray transients. It is emphasized that the temporal resolution of the setup is determined by the RC-constant of the transimpedance amplifier or the data acquisition system (e.g., the input impedance of an oscilloscope). Figure 11 shows a typical instability signal measured with the JYFL 14 GHz ECRIS using a BGO scintillator coupled with a Na-doped CsI (300–600 nm) current-mode photomultiplier tube. The PMT output was measured with an oscilloscope through a transimpedance amplifier, which converted the PMT current output to the amplified voltage signal. As can be seen in this figure, the decay time of the scintillator setup, about 100 μs, is much longer than the characteristic time of the instability induced electron burst (0.1–1 μs order of magnitude). This highlights the fact that the temporal resolution of the scintillator setup is determined by the RC constant of the signal processing part of the setup. This needs to be taken into account during the data analysis and when drawing conclusions from the measurements.

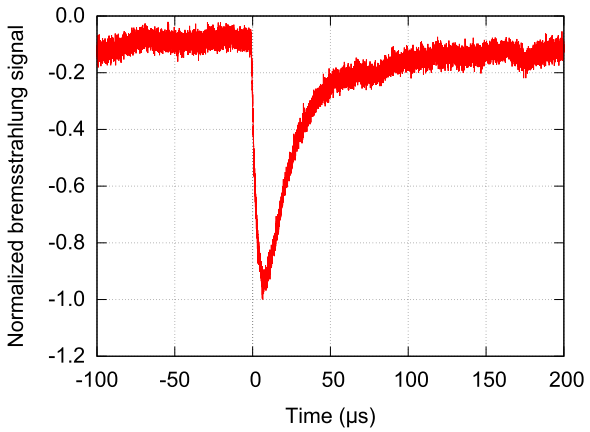

FIG. 11. An example of typical instability-induced bremsstrahlung signal measured with a BGO scintillator coupled with a current-mode PMT (with a Na-doped CsI photocathode). The data were measured with JYFL 14 GHz ECRIS.

A scintillator setup provides a simple and convenient way to monitor whether the plasma is stable or unstable based on the presence of instability-induced x-ray bursts, which can be used to define the stable/unstable plasma regimes and the parameters affecting the instability threshold (see, for example, Ref. 7). The scintillator setup has often been used as a secondary instability diagnostics parallel with the primary diagnostics (e.g., microwave diagnostics). The 100 μs signal decay time of the scintillator setup is adequate to obtain information about the repetition rate of the instabilities,[7] and thus, the setup can be used to study, e.g., the relation between the instability repetition rate and the magnitude of the instability events, as has been demonstrated by Bhaskar *et al.*[45] Reference 9 discusses measurements where the occurrence of plasma instabilities were monitored with two BGO x-ray detectors placed inside the axial radiation cones at the injection and the extraction sides of the GTS ion source at GANIL. At each instability event, the scintillators displayed a constant signal ratio when the relative strengths of the signals were compared, suggesting that the instability event expels electrons from the plasma "globally," not directionally.

B. Energy sensitive semiconductor detectors

While the scintillator is a good choice for monitoring the plasma stability, repetition rate of instabilities, and the magnitude of instability-induced electron bursts, a semiconductor detector, such as high-purity Ge-detector or CdTe detector, is required for the measurement of the bremsstrahlung energy spectrum.

The energy needed to produce a free electron and hole pair in semiconductors is well-known, and the number of produced pairs is proportional to the energy of the radiation interacting with the semiconductor material. Under the influence of the applied electric field, the free electrons will result in a pulse, which is converted to a voltage signal by a preamplifier. The amplitude of the detected voltage signal depends on the energy of the incoming photon, and therefore, its energy can be defined when a proper energy calibration of the detector is done. Further information about different factors affecting the measured spectrum, such as attenuation and scattering of radiation in the surrounding structures, efficiency corrections, etc., can be found, for example, from Ref. 46.

If not correctly dealt with, the results can be distorted by the detector dead-time and pile-up events. The dead-time is the period after an event when the detector system is not able to detect another incoming photon (signal processing time). In a pile-up event, two or more photons are detected so close to each other in time that the detector system processes them incorrectly as a single event with their combined energy. To assure proper functioning of the bremsstrahlung measurement setup, the dead-time must be minimized (e.g., by collimation) and pile-up events flagged and vetoed by the digital signal processing.

Published under an exclusive license by AIP Publishing

The bremsstrahlung photon flux associated with instability events is often so high that only pile-up events are recorded, which is a serious limitation of energy sensitive detectors for instability diagnostics. Thus, only the temporally averaged bremsstrahlung spectrum can be measured reliably in the unstable regime. For this reason, the number of instability studies where semiconductor detectors have been used to obtain information about the instability induced bremsstrahlung burst is low. In 2009, a high-purity germanium (HPGe) detector was used by Ropponen *et al.* to study the magnetic field effect on the time evolution of high-energy bremsstrahlung radiation.[47] The data were collected using 2 ms time intervals ,and 750 spectra were recorded and combined to acquire an adequate amount of statistics for the data analysis. It was found, for example, that the total number of bremsstrahlung radiation had oscillations at high magnetic field values. It was suggested that the plasma becomes unstable as a result of the improved electron heating efficiency caused by the low magnetic field gradient, but no solid explanation was given.

Some experimental campaigns probing the unstable plasma regime have been performed in the time-averaged mode using HPGe and cadmium-tellurium (CdTe) semiconductor detectors.[18,19,40] These studies have revealed that the shape of the temporally averaged bremsstrahlung spectrum does not significantly change between the stable and unstable plasma regimes. The result can be explained by the short duration (at the level of microseconds) of the instability burst and the properties of the detector system. The typical instability repetition rate is 0.1–1 kHz (order of magnitude), meaning that the duration of the instability burst covers 0.01%–1% of the total instability period. During the instability burst, the flow rate of the electrons can be 1–2 orders of magnitudes higher compared to the stable plasma. As mentioned earlier, this may result in a remarkable distortion of the detected signals due to pile-up events. These factors can explain why no significant changes are observed in the bremsstrahlung spectrum in the time-averaged experiments. These issues could be solved by using a more sophisticated collimator setup to avoid dead-time and pile-up during the instability-induced electron bursts and by triggering the bremsstrahlung measurement to include only the instability transient. This approach requires that a sufficient amount of instability periods are recorded to collect enough statistics to construct the bremsstrahlung spectrum.

The main advantages and findings of the instability-related bremsstrahlung studies can be summarized as follows: (1) The scintillator is an effective way to study the amplitude and the repetition rate of plasma instabilities as well as to determine the instability thresholds and the parameter space for stable plasma operation. (2) The scintillator setup is a simple and fairly low-cost method to monitor plasma instabilities non-invasively. (3) The time-averaged bremsstrahlung energy spectrum is not significantly influenced by the onset of instabilities, and thus, it cannot be used to determine the transition from stable to unstable plasma.[40]

V. ION FLUX

The sudden increase in electron losses due to the instability onset causes a disturbance to the plasma ion population. The diagnostic techniques that have been employed to study the instabilities through the resulting ion flux from the plasma include (a) the use of the ion source biased disk as a probe for ion losses, (b) measurement and analysis of the extracted beam current, and (c) determination of the plasma potential variation from the changes in the extracted beam energy spread. The use of the biased disk to study the ion flux is not discussed further here, as the topic is already presented in detail in Sec. III, and the same measurement setup is also applicable for ion studies. The other ion flux related techniques are summarized in the following text. In addition, the detection of plasma emitted visible light to probe the behavior of plasma ion population during instabilities is discussed briefly at the end of the section.

A. Extracted beam current

The plasma instabilities cause periodic oscillations of the extracted ion beam current, and arguably the simplest diagnostic technique to study this behavior is to monitor the temporal behavior of the beam current with a Faraday cup downstream from the m/q separation to allow individual study of the different extracted ion species and charge states. Consequently, this method has been employed widely in published ECRIS plasma instability studies (see, e.g., Refs. 7, 12, 17, 19, 37, and 48–52). As relatively similar measurement systems for temporal beam current monitoring have been used in many studies, the following text focuses on summarizing the main features required of such a system to accurately detect the instability-induced beam current variations and the main considerations associated with them rather than individually presenting each setup variation.

The first consideration is to ensure that the measurement system has a sufficient temporal resolution to accurately measure the influence of the plasma instabilities on the ion beam. When a Faraday cup is used for the current measurement, the cup structure itself, the cables that connect it to the data acquisition system, and other possible elements on the signal path increase the RC constant of the measurement setup. Determining (and mitigating) this influence in the setup is essential as it will limit how precisely the fine structure of the beam current variation can be detected. Connecting the Faraday cup current output directly to a fast transimpedance amplifier placed close to the cup and recording the amplifier voltage output with an oscilloscope or some other high sample rate data acquisition system has proven to be a good solution for this.[37] The sampling rate of the data acquisition system itself sets a second limitation for the temporal resolution, especially because historically many current measurement systems have been developed for longer term monitoring of the beam current behavior and, consequently, may lack the required temporal resolution to detect the instability-induced current variations which typically occur in the millisecond time scales. Similarly, such systems might impose averaging on the measured signal, which obscures the real temporal behavior. As a result, the onset of the instabilities is observed as a reduction of the average measured beam current (for high charge state ions), but the real temporal variation is not seen in the measured current.

The occurrence of plasma instabilities has a charge state dependent effect on the extracted beam current behavior.[7,8] The general observed trend is that beam currents of high charge state ions exhibit a sudden decrease at the onset of the instability, followed by a recovery period. The low charge state ions exhibit the opposite behavior with a temporary increase in the beam currents. As an example, Fig. 12 presents measured beam currents of $^{16}O^{3+}$

Published under an exclusive license by AIP Publishing

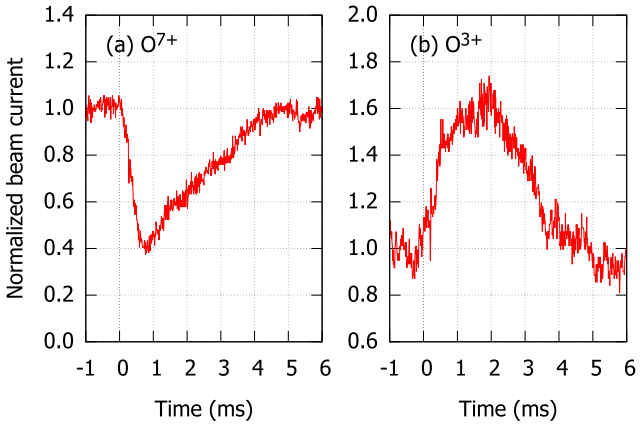

FIG. 12. Examples of (a) $^{16}O^{7+}$ and (b) $^{16}O^{3+}$ beam current transients following a plasma instability event at $t = 0$. In both cases, the beam currents are normalized to the value preceding the instability onset. The presented cases were measured with the JYFL 14 GHz ECRIS.

and $^{16}O^{7+}$ after a plasma instability event. This behavior is further demonstrated in Fig. 13, which shows a comparison of argon charge state distributions (CSDs) measured with stable and unstable plasma conditions. It is seen that with unstable plasma, the CSD shifts to lower charge states, and consequently, the average charge state of the extracted beam decreases. The fast temporal variation of the beam current caused by the instabilities is also captured in the measurement, manifesting as large current variations on the measured CSD peaks.

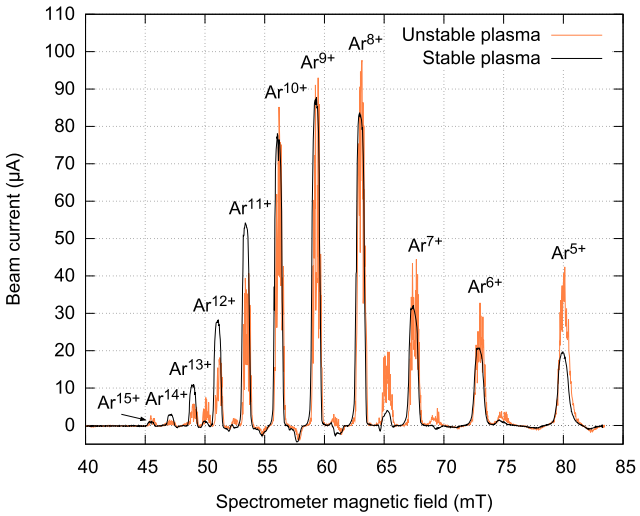

FIG. 13. Argon charge state distributions measured in stable and unstable plasma regimes. The transition from stable to unstable plasma was realized by increasing the ion source axial magnetic field over the instability threshold value. It is noted that argon charge states 5+, 10+, and 15+ include contribution from residual oxygen charge states. The presented cases were measured with the JYFL 14 GHz ECRIS.

B. The energy spread of the extracted ion beam

As has been discussed earlier, the onset of the plasma instability is accompanied by an abrupt increase in the plasma ambipolar potential. As a result, a significant energy spread is introduced to the energy of the extracted ions, which alters the ion trajectories through the spectrometer magnet. This consequently influences the beam current measurement downstream from the spectrometer, as the monitored ion species is deviated from its intended path during the potential shift. References 8 and 9 present results from studies attempting to quantify this potential shift by measuring the extracted beam energy variation with the ion source spectrometer magnet. The approach is similar to the technique described in Sec. III for the determination of the escaping electron energy distribution, i.e., the spectrometer magnetic field is varied in steps and the temporal behavior of the ion current downstream from the spectrometer is recorded at each step. Reconstructing the resulting waveforms into a time vs B field plot provides a way to determine how much a chosen ion species current is spread in B field during the instability event, from which the temporal variation of the beam energy spread $\Delta E/E$, corresponding to the variation of the plasma potential, can be calculated. An example is presented in Fig. 14. The results presented in Refs. 8 and 9 show that the plasma potential shift occurs immediately after the instability onset, and for a few microseconds, the plasma potential can reach transient values in excess of 1 kV. After the initial peak, the influence of the potential shift was visible in the measurements for some tens of microseconds. Furthermore, the energy spread measurement reveals that the ion source (positive) high voltage power supply is not capable of handling the surge of electrons to the chamber walls causing a voltage droop seen in Fig. 14 as a ~1% beam energy shift toward lower energies (for more examples see Ref. 9). The variation of the plasma potential and the consequent losses of energetic ions release impurities from the plasma chamber walls through desorption and sputtering, which introduces impurity elements into the plasma and the extracted beam.[8,9,12]

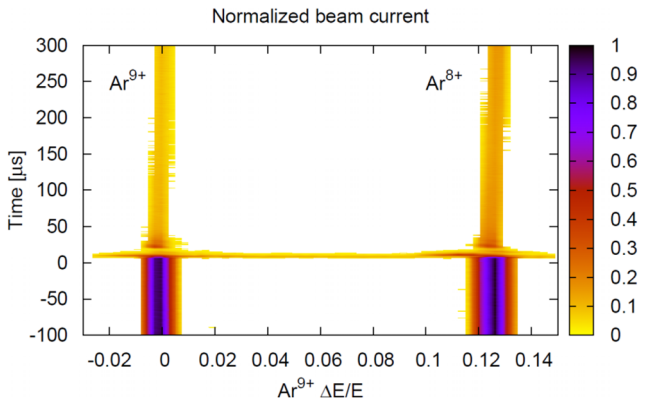

FIG. 14. Temporal variation of Ar^{9+} ion beam energy spread measured with the ion source spectrometer magnet. The $t = 0$ corresponds to the instability onset, and the x-axis represents the magnetic field sweep of the spectrometer. The false color scale represents the beam current normalized to the maximum intensity of Ar^{9+}. Reproduced from Tarvainen *et al.*, Rev. Sci. Instrum. **87**, 02A703 (2016) with the permission of AIP Publishing.

Published under an exclusive license by AIP Publishing

C. Plasma emitted visible light

The impact of the instabilities on the ion population can be studied by measuring the plasma emitted light. Reference 7 describes a diagnostic system composed of a visible light collector setup coupled with a photomultiplier tube (PMT) to measure the variation in the visible light intensity emitted by the plasma in the unstable regime. The light was measured through a viewport in the injection plug of an ECR ion source, which provided an off-axis view into the plasma chamber. The light from the plasma was focused into an optical coupler with a set of lenses and converted into electrical signal with the PMT. The PMT sets the range for the measured light wavelength and the temporal resolution of the measurement. As an example, in the case of Ref. 7, these were reported to be 300–600 nm and <4 μs, respectively. Experiments with oxygen plasma[7] have shown that at the onset of the instability, the visible light signal exhibits an abrupt increase, which is followed by a decay that lasts for several milliseconds, and the initial increase occurs at the same time as the instability-induced burst of bremsstrahlung. As the measured visible light wavelength range is dominated by emission lines of neutrals and low oxygen charge states, the variation in the light signal has been associated with changing conditions in the neutral gas balance and/or changes in the charge state distribution of the oxygen ions,[7] especially as the instabilities are known to also introduce impurities into the plasma from the chamber walls.[12,52]

The main highlights of experimental results obtained with ion based diagnostics techniques can be summarized as follows: (1) The instability onset causes an abrupt disturbances to the extracted ion beam currents with ms-scale recovery times.[7,17] (2) The influence of the instabilities on the ion beam currents is charge state dependent, with the high charge states exhibiting a sudden drop in current, whereas the low charge state currents are increased following an

TABLE I. Comparison of different diagnostic techniques for minimum-*B* ECR ion source plasma instabilities.

Diagnostic technique	Advantages	Disadvantages and practical limitations
	Microwave emission techniques	
Microwave diode	Easy to implement (low-cost) Provides temporal information of emission power	No frequency information
Spectrum analyzer	Measurement of emission frequencies Provides real-time information	Not temporally resolved
High-bandwidth oscilloscope	Time-resolved measurement of emission frequencies	Requires extensive data post-processing Often prohibitively expensive
	Electron detection techniques	
Biased disk	Direct measurement of plasma expelled electrons Also provides information about expelled ions	No energy information
PIN diode + filters	Time-resolved measurement of electron flux Provides discrete EED of escaping electrons	EED discretization set by number of filters Energy range limited by diode properties Sensitive to x-rays
Faraday cup + filters	Provides discrete EED of escaping electrons	EED discretization set by number of filters
Electron spectrometer	Provides continuous EED of escaping electrons	Requires careful calibration and corrections Requires data post-processing
	Bremsstrahlung techniques	
X-ray scintillator + PMT	Easy to implement (low-cost) Provides temporal information of emission power	No energy information
Energy sensitive detector	Provides energy information	Complexity of time-resolved measurements No real-time information (long data acq. time) Can be fairly expensive
	Ion detection techniques	
Biased disk	Direct measurement of plasma expelled ions Also provides information about expelled electrons	No energy information No ion species information
Extracted beam current (FC)	Easy to implement (low-cost) Provides time-resolved ion species information	Affected by the RC constant
Plasma potential from extracted beam	Time-resolved measurement of plasma potential shift	Requires data post-processing
Plasma emitted total visible light	Time-resolved information about changing ion and neutral conditions in plasma	Not wavelength-resolved

Published under an exclusive license by AIP Publishing

instability event. As a result the CSD of the extracted beam shifts toward lower charge states.[7] (3) The energy spread of the extracted beam experiences a sudden increase for some μs following the onset of plasma instability, which indicates a shift of >1 kV in the ion source plasma potential as a result of the instability-induced electron losses.[8,9] (4) The visible light emitted by the plasma provides a way to probe the changing plasma composition (neutrals and ions) during instabilities.[7]

VI. DISCUSSION

The different diagnostics techniques for minimum-B ECRIS plasma instabilities that have been discussed in this paper are summarized in Table I with the main advantages and disadvantages/limitations that are associated with each technique.

A. Implications of ECRIS plasma instabilities

Diagnostics of plasma instabilities in minimum-B ECR ion sources are relevant for their operation as injectors to heavy ion accelerators, where instabilities cause periodic oscillation of the extracted beam, and for the design of next generation ion sources with >28 GHz plasma heating frequencies. This is because the plasma instabilities often restrict the parameter space available for the optimization of high charge state ion beam currents. This is especially true for the B_{min}, which has been demonstrated to be the most influential ion source (magnetic field) parameter affecting the EED[42,53] and the transition from the stable to unstable regime.[7]

The threshold B_{min} of the transition to unstable regime is often found at B_{min}/B_{ECR} = 0.7–0.8, which prohibits operating the ion source at the optimum B_{min} of 0.8 (for high charge state production), derived from the semi-empirical scaling laws of the ECRIS magnetic field.[54] Figure 15 shows examples of high charge state beam currents recorded with the JYFL 14 GHz ECRIS as a function of the B_{min}/B_{ECR}-ratio. It is seen that the extracted beam currents increase until the transition to unstable regime occurs. In the unstable regime, the plasma confinement is periodically perturbed at temporal interval shorter than the production time[55] or cumulative confinement time[56] of the high charge state ions, which suppresses their densities in the plasma as well as their escape flux (beam current). The instability threshold B_{min}/B_{ECR} depends on the plasma composition. The threshold B_{min} increases with the mass of the plasma gas, i.e., by ~5%–10% from helium to xenon.[57] The effect is attributed to the increased rate of inelastic collisions in heavy element discharges and the subsequent increase in the instability damping rate. The mass (or Z) dependence of the instability threshold implies that one should expect the said B_{min}-scaling to depend on the plasma species and composition (e.g., gas mixing conditions).

The instabilities have implications on the interpretation of ECRIS B-field scaling experiments at high frequency[54] and pulsed operation of ECR ion sources in the afterglow mode. This stems from the temporal delay between the plasma breakdown and the appearance of the instabilities, which has been found to be on the order of 10–100 ms for a 14 GHz ECRIS, depending strongly on the magnetic field settings and neutral gas pressure.[51] The reported time scale matches well with the observed electron heating time

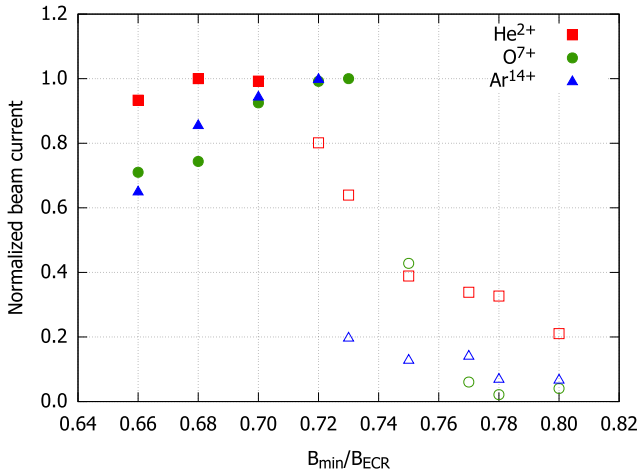

FIG. 15. Behavior of He^{2+}, O^{7+}, and Ar^{14+} beam currents with increasing B_{min}/B_{ECR}-ratio, measured with the JYFL 14 GHz ECRIS. The solid and open symbols represent stable and unstable plasma conditions, respectively. Reproduced from Tarvainen *et al.*, Rev. Sci. Instrum. **87**, 02A701 (2016) with the permission of AIP Publishing.

and evolution of the high energy EED.[47] The B-field scaling experiments reported in Ref. 54 were conducted in the pulsed mode (with unspecified pulse length). It is therefore important to note that above the optimum B_{min}-value, the beam current pulses in Ref. 54 appear somewhat noisy, which could be interpreted as a sign of the ion source operating in the unstable regime. If that was the case, the scaling law experiments can be argued to strengthen the position of the instabilities limiting ECRIS performances. On the other hand, the B-field scaling in continuous operation could be different as it would be important to allow enough time for the EED to evolve and instabilities to develop in the pulsed mode at each B_{min}. In pulsed (afterglow) operation, B_{min} is often set higher than B_{min}/B_{ECR} = 0.8, which is often found to be the upper limit in continuous operation.[58] This is because the microwave pulse length is short enough, preventing the development of instabilities at high B_{min}, i.e., above the threshold found in the continuous microwave injection mode.

The plasma instabilities have also been found to limit the efficiencies of ECRIS charge breeders and increase the beam currents of impurity ions extracted from them.[12,52] This is because the instabilities prevent optimizing the magnetic field strength and the plasma potential fluctuations cause increased sputtering of the plasma chamber wall material.

B. Instabilities in pulsed operation mode

Diagnostics campaigns in the pulsed (microwave injection) mode of an ECRIS have been carried out by many authors. The applied diagnostics techniques include, e.g., time-resolved bremsstrahlung measurements,[47,59] pick-up loops to measure the plasma diamagnetism,[60] and optical emission measurements.[61] These diagnostics are used for determining the characteristic time scale of the build-up and decay of the plasma energy content. It has been found that kinetic instabilities have a profound effect on the plasma decay characteristics.[31] Most importantly, they explain the

Published under an exclusive license by AIP Publishing

abrupt perturbations of the extracted ion current during the plasma decay after the instant "afterglow" ion current peak exhibited by the high charge state ions following the trailing edge of the microwave pulse. The sequential drops and partial recoveries of the ion beam current are accompanied by microwave and bremsstrahlung emission, which is a fingerprint of the maser-type instability. An example of this correlation is presented in Fig. 16. The energy carried by each burst of microwave and bremsstrahlung emission associated with the afterglow-instability is significantly higher in comparison to cw-mode instabilities. This is because the anisotropy of the EED is stronger during the plasma decay as the cold, collisional electrons are the first ones to exit the confinement leading to a short enhancement of the ion beam current (often called the afterglow-peak), leaving behind the well-confined hot electrons. The higher $N_{e,hot}/N_{e,cold}$-ratio leads to increased growth rate of the instability.[13] Furthermore, in the decaying plasma instabilities are the only notable loss mechanism of hot electrons as opposed to the cw microwave injection mode where rf scattering contributes to the losses of high energy electrons.[42] The implication is that during the plasma decay, the instability onsets tend to be more violent than in the cw-mode, which means that the instability diagnostics must be better protected against overvoltages and current surges damaging them.

C. Suppression of ECRIS plasma instabilities by two-frequency heating

In Subsections VI A and VI B, we have described that kinetic instabilities limit the parameter space of ECRIS optimization by reducing the extracted currents of high charge state ions, increasing the energy spread of the ion beams and releasing contaminants from the plasma chamber walls. Thus, the motivation for suppressing the instabilities is apparent. Multiple frequency heating is one of the most effective techniques to improve the performance of ECR ion sources (see the paper by Vondrasek *et al.* in this Special Issue). It has been discovered that the beneficial effect of two-frequency heating is connected to enhanced plasma stability and suppression of kinetic instabilities.[48,50] The effect is demonstrated in Fig. 17, showing the O^{6+} beam current and x-ray power flux recorded with the JYFL 14 GHz ECRIS in single and double frequency heating modes. The periodic ripple observed in the single frequency heating mode disappears and the beam current of O^{6+} increases when the secondary microwave source is turned on. Furthermore, the fluctuations of x-ray power flux disappear in the two frequency operation mode, indicating the suppression of the instability.

Another example of the two-frequency heating suppressing the instabilities and altering the energy distribution of the electrons escaping through the extraction aperture is shown in Fig. 18. When the secondary frequency is applied, the plasma becomes quiescent and the average energy of the escaping electrons increases, which is interpreted as a sign of increased rf scattering rate of high energy electrons into the magnetic loss cone. The increased rf scattering stabilizes the plasma as it enhances the loss rate of the energy stored in the EED, which would otherwise dissipate via instability-induced microwave emission and particle losses.

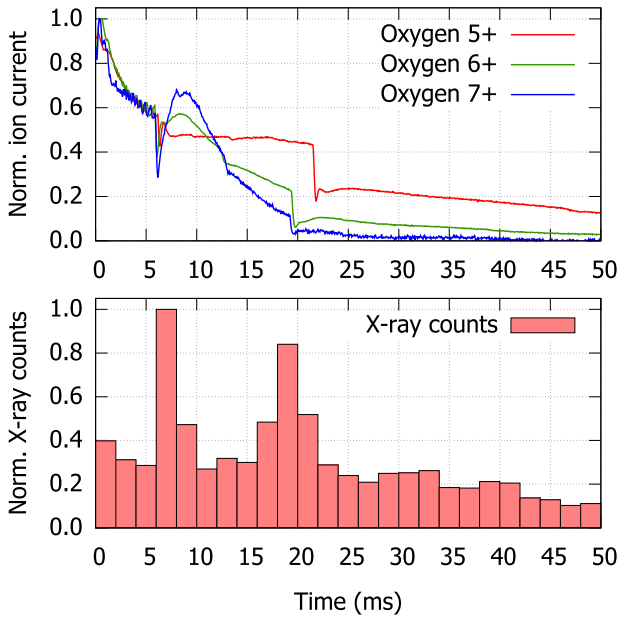

FIG. 16. Normalized beam currents of selected oxygen charge states and bremsstrahlung count rate measured during the afterglow plasma decay. Microwaves are switched off at $t = 0$. The sudden drops exhibited by the ion currents correlate with the bremsstrahlung bursts which indicate the onset of instabilities. Reproduced from Izotov *et al.*, Phys. Plasmas **19**, 122501 (2012) with the permission of AIP Publishing.

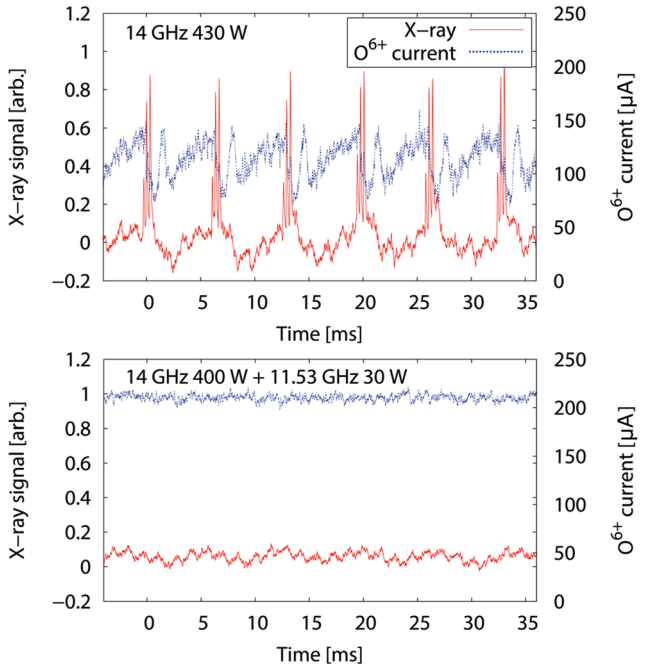

FIG. 17. The effect of two-frequency heating on suppressing plasma instabilities. (Top) The O^{6+} beam current and x-ray power flux recorded in the single frequency heating mode (14 GHz) and unstable plasma. (Bottom) Stable plasma with the same ion source settings and equal total rf power with double frequency heating (14 and 11.56 GHz). Reproduced from Skalyga *et al.*, Phys. Plasmas **22**, 083509 (2015) with the permission of AIP Publishing.

Published under an exclusive license by AIP Publishing

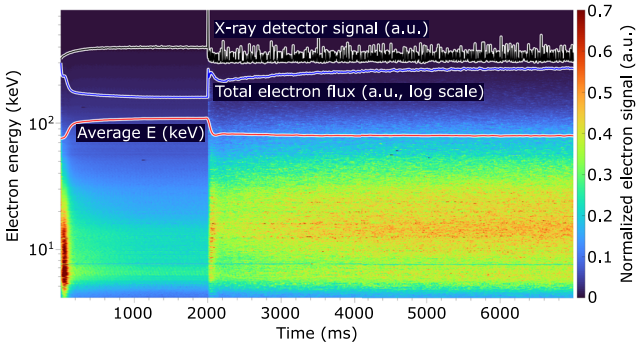

FIG. 18. The stabilizing effect of the two-frequency heating as seen on the measured energy distribution of axially lost electrons and the emitted x-rays. The time evolution of the calculated total electron flux and the average electron energy is also shown. An unstable plasma, sustained with continuous microwave heating of 250 W at 14 GHz, is stabilized by adding a secondary pulsed heating frequency (11.56 GHz, 100 W) at $t = 0$. The secondary frequency is turned off at $t = 2000$ ms, i.e., the pulse pattern is 2 s ON/5 s OFF. The transition between the two regimes occurs within the first 100–200 ms after the step-change.

D. Diagnostics development and experimental needs

In Secs. II–V, we have established the state-of-the-art of the instability-related diagnostics techniques applicable for minimum-B ECR ion sources. However, there are still numerous reasons to further develop the listed diagnostics techniques as well as new methods to probe the physics of the instabilities.

Most of the experiments on ECRIS instabilities have been conducted with room-temperature sources operating at frequencies up to 14.5 GHz. For complete understanding of the instability-physics, especially their trigger mechanism, it would be beneficial to extend similar experiments, e.g., time-resolved emission frequency diagnostics and (escaping) electron energy distribution measurements, to superconducting ion sources operating at >20 GHz frequencies.

Specific examples of diagnostics development needs include (i) internal rf probes capable of measuring emission frequencies below the waveguide cutoff to probe the role of rf scattering on the formation of the unstable EED,[42] (ii) measurements with diamagnetic coils revealing the fraction of plasma energy content lost in each instability onset (through a comparison to plasma ignition transient), and (iii) further development of wavelength-resolved and time-resolved optical emission detection based on bandpass filters and photodiodes[62] and/or monochromator coupled with a CCD array[63,64] revealing information on instability-induced ion losses and fluctuations of the charge state distribution and ion temperature within the plasma volume (not only in the extracted beam).

ACKNOWLEDGMENTS

This work has been supported by the Academy of Finland Project funding (No. 315855) and the University of Grenoble Alpes under the EMERGENCE program. The data processing was supported by the Russian Science Foundation (Grant No. 19-12-00377). We would also like to thank Risto Kronholm of JYFL for providing the necessary technical assistance.

AUTHOR DECLARATIONS

Conflict of Interest

The authors have no conflicts to disclose.

DATA AVAILABILITY

Data sharing is not applicable to this article as no new data were created or analyzed in this study, with the exception of Figs. 1, 3, 4, 5, 11, 12, 13, and 18, for which the data that support the findings of this study are available within the article.

REFERENCES

[1] R. Geller, *Electron Cyclotron Resonance Ion Sources and ECR Plasmas* (Taylor & Francis, 1996).
[2] T. A. Antaya, "The superconducting electron cyclotron resonance 6.4 GHz high-B mode and frequency scaling in electron cyclotron resonance ion sources," Rev. Sci. Instrum. **65**, 1723 (1994).
[3] C. Barué, M. Lamoureux, P. Briand, A. Girard, and G. Melin, "Investigation of hot electrons in electron-cyclotron-resonance ion sources," J. Appl. Phys. **76**, 2662 (1994).
[4] G. Douysset, H. Khodja, A. Girard, and J. P. Briand, "Highly charged ion densities and ion confinement properties in an electron-cyclotron-resonance ion source," Phys. Rev. E **61**, 3015 (2000).
[5] S. V. Golubev and A. G. Shalashov, "Cyclotron-resonance maser driven by magnetic compression of rarefied plasma," Phys. Rev. Lett. **99**, 205002 (2007).
[6] A. G. Shalashov, E. D. Gospodchikov, and I. V. Izotov, "Electron-cyclotron heating and kinetic instabilities of a mirror-confined plasma: The quasilinear theory revised," Plasma Phys. Controlled Fusion **62**, 065005 (2020).
[7] O. Tarvainen, I. Izotov, D. Mansfeld, V. Skalyga, S. Golubev, T. Kalvas, H. Koivisto, J. Komppula, R. Kronholm, J. Laulainen, and V. Toivanen, "Beam current oscillations driven by cyclotron instabilities in a minimum-B electron cyclotron resonance ion source plasma," Plasma Sources Sci. Technol. **23**, 025020 (2014).
[8] O. Tarvainen, T. Kalvas, H. Koivisto, J. Komppula, R. Kronholm, J. Laulainen, I. Izotov, D. Mansfeld, V. Skalyga, V. Toivanen, and G. Machicoane, "Limitation of the ECRIS performance by kinetic plasma instabilities (invited)," Rev. Sci. Instrum. **87**, 02A703 (2016).
[9] O. Tarvainen, R. Kronholm, T. Kalvas, H. Koivisto, I. Izotov, V. Skalyga, V. Toivanen, and L. Maunoury, "The biased disc of an electron cyclotron resonance ion source as a probe of instability-induced electron and ion losses," Rev. Sci. Instrum. **90**, 123303 (2019).
[10] U. Amaldi, R. Bonomi, S. Braccini, M. Crescenti, A. Degiovanni, M. Garlasché, A. Garonna, G. Magrin, C. Mellace, P. Pearce, G. Pittà, P. Puggioni, E. Rosso, S. V. Andrés, R. Wegner, M. Weiss, and R. Zennaro, "Accelerators for hadrontherapy: From Lawrence cyclotrons to linacs," Nucl. Instrum. Methods Phys. Res., Sect. A **620**, 563–577 (2010).
[11] A. Denker, H. Homeyer, H. Kluge, and J. Opitz-Coutureau, "Industrial and medical applications of high-energy ions," Nucl. Instrum. Methods Phys. Res., Sect. B **240**, 61–68 (2005).
[12] O. Tarvainen, J. Angot, I. Izotov, V. Skalyga, H. Koivisto, T. Thuillier, T. Kalvas, and T. Lamy, "Plasma instabilities of a charge breeder ECRIS," Plasma Sources Sci. Technol. **26**, 105002 (2017).
[13] S. V. Golubev and A. G. Shalashov, "Cyclotron-resonance maser with adiabatic magnetic pumping in a low-density plasma," JETP Lett. **86**, 91–97 (2007).
[14] A. G. Shalashov, S. V. Golubev, E. D. Gospodchikov, D. A. Mansfeld, and M. E. Viktorov, "Interpretation of complex patterns observed in the electron-cyclotron instability of a mirror confined plasma produced by an ECR discharge," Plasma Phys. Controlled Fusion **54**, 085023 (2012).
[15] R. C. Garner, M. E. Mauel, S. A. Hokin, R. S. Post, and D. L. Smatlak, "Warm electron-driven whistler instability in an electron-cyclotron-resonance heated, mirror-confined plasma," Phys. Rev. Lett. **59**, 1821–1824 (1987).

Published under an exclusive license by AIP Publishing

[16]R. C. Garner, M. E. Mauel, S. A. Hokin, R. S. Post, and D. L. Smatlak, "Whistler instability in an electron-cyclotron-resonance-heated, mirror-confined plasma," Phys. Fluids B **2**, 242 (1990).
[17]O. Tarvainen, V. Toivanen, H. Koivisto, J. Komppula, T. Kalvas, C. Lyneis, and M. Strohmeier, "An experimental study of ECRIS plasma stability and oscillation of beam current," in Proceedings of the 20th International Workshop on ECR Ion Sources, Sydney, Australia, 2012.
[18]J. B. Li, L. X. Li, B. S. Bhaskar, V. Toivanen, O. Tarvainen, D. Hitz, L. B. Li, W. Lu, H. Koivisto, T. Thuillier, J. W. Guo, X. Z. Zhang, H. Y. Zhao, L. T. Sun, and H. W. Zhao, "Effects of magnetic configuration on hot electrons in a minimum-B ECR plasma," Plasma Phys. Controlled Fusion **62**, 095015 (2020).
[19]B. Isherwood, E. Pozdeyev, G. Machicoane, J. Stetson, and D. Neben, "Plasma instability studies of SUSI 18 GHz source," in *Proceedings of 23rd Workshop on ECR Ion Sources* (JACoW, Catania, Italy, 2018), pp. 157–161; available at https://accelconf.web.cern.ch/ecris2018/papers/wea3.pdf.
[20]E. Naselli, D. Mascali, M. Mazzaglia, S. Biri, R. Rácz, J. Pálinkás, Z. Perduk, A. Galatá, G. Castro, L. Celona, S. Gammino, and G. Torrisi, "Impact of two-close-frequency heating on ECR ion source plasma radio emission and stability," Plasma Sources Sci. Technol. **28**, 085021 (2019).
[21]M. Viktorova, A. Shalashov, S. Golubev, E. Gospodchikov, D. Mansfeld, A. Vodopyanov, and V. Zaitsev, "Kinetic instabilities in a mirror-confined plasma sustained by high-power microwave radiation," AIP Conf. Proc. **1771**, 030005 (2016).
[22]I. Izotov, O. Tarvainen, D. Mansfeld, V. Skalyga, H. Koivisto, T. Kalvas, J. Komppula, R. Kronholm, and J. Laulainen, "Microwave emission related to cyclotron instabilities in a minimum-B electron cyclotron resonance ion source plasma," Plasma Sources Sci. Technol. **24**, 045017 (2015).
[23]I. Izotov, T. Kalvas, H. Koivisto, R. Kronholm, D. Mansfeld, V. Skalyga, and O. Tarvainen, "Broadband microwave emission spectrum associated with kinetic instabilities in minimum-B ECR plasmas," Phys. Plasmas **24**, 043515 (2017).
[24]V. Skalyga, I. Izotov, D. Mansfeld, O. Tarvainen, T. Kalvas, J. Laulainen, R. Kronholm, J. Komppula, and H. Koivisto, "Microwave emission from ECR plasmas under conditions of two-frequency heating induced by kinetic instabilities," AIP Conf. Proc. **2011**, 020015 (2018).
[25]J. Orpana, O. Tarvainen, T. Kalvas, H. Koivisto, R. Kronholm, J. Laulainen, I. Izotov, D. Mansfeld, and V. Skalyga, "Measurement of microwave frequencies emitted by instabilities of ECRIS plasma with waveguide filters and microwave sensitive diodes," in Proceedings of the 22nd International Workshop on ECR Ion Sources, Busan, Korea, 2016.
[26]Data sheet for Keysight N9042B UXA X-Series Signal Analyzer, https://www.keysight.com/us/en/assets/3121-1037/data-sheets/N9042B-UXA-X-Series-Signal-Analyzer-Multi-touch.pdf, 2021; accessed 12 October 2021.
[27]Data sheet for Keysight FieldFox Handheld Analyzers, https://www.keysight.com/fi/en/assets/7018-06516/data-sheets/5992-3702.pdf, 2021; accessed 12 October 2021.
[28]I. Izotov, T. Kalvas, H. Koivisto, J. Komppula, R. Kronholm, J. Laulainen, D. Mansfeld, V. Skalyga, and O. Tarvainen, "Cyclotron instability in the afterglow mode of minimum-B ECRIS," Rev. Sci. Instrum. **87**, 02A729 (2016).
[29]Data sheet for Keysight Infiniium UXR-Series Oscilloscopes, https://www.keysight.com/us/en/assets/7018-06242/data-sheets/5992-3132.pdf, 2021; accessed 12 October 2021.
[30]H. Zhao, L. Sun, J. Guo, W. Lu, D. Xie, D. Hitz, X. Zhang, and Y. Yang, "Intense highly charged ion beam production and operation with a superconducting electron cyclotron resonance ion source," Phys. Rev. Accel. Beams **20**, 094801 (2017).
[31]D. Mansfeld, I. Izotov, V. Skalyga, O. Tarvainen, T. Kalvas, H. Koivisto, J. Komppula, R. Kronholm, and J. Laulainen, "Dynamic regimes of cyclotron instability in the afterglow mode of minimum-B electron cyclotron resonance ion source plasma," Plasma Phys. Controlled Fusion **58**, 045019 (2016).
[32]A. Vodopyanov, S. Golubev, A. Demekhov, V. Zorin, D. Mansfeld, S. Razin, and V. Trakhtengerts, "Laboratory modeling of nonstationary processes in space cyclotron masers: First results and prospects," Plasma Phys. Rep. **31**, 927–937 (2005).
[33]A. G. Shalashov, A. V. Vodopyanov, S. V. Golubev, A. G. Demekhov, V. G. Zorin, D. A. Mansfeld, and S. V. Razin, "Maser based on cyclotron resonance in a decaying plasma," JETP Lett. **84**, 314–319 (2006).
[34]A. V. Vodopyanov, S. V. Golubev, A. G. Demekhov, V. G. Zorin, D. A. Mansfeld, S. V. Razin, and A. G. Shalashov, "Observation of pulsed fast electron precipitations and the cyclotron generation mechanism of burst activity," J. Exp. Theor. Phys. **104**, 296–306 (2007).
[35]S. Golubev, D. Mansfeld, A. Shalashov, and A. Vodopyanov, "Plasma magneto-compressional cyclotron maser," in Proceedings of the 35th International Conference on Infrared, Millimeter and THz Waves, Houston, USA, 2010.
[36]M. Viktorov, S. Golubev, E. Gospodchikov, I. Izotov, D. Mansfeld, A. Shalashov, and A. Vodopyanov, "Generation of wideband electromagnetic radiation under magnetic compression of a mirror-confined plasma produced by ECR discharge," in *Proceedings of 8th International Workshop on Strong Microwaves and Terahertz Waves: Sources and Applications* (IAP RAS, Nizhny Novgorod, St. Petersburg, Russia, 2011), p. 204.
[37]I. Izotov, D. Mansfeld, V. Skalyga, V. Zorin, T. Grahn, T. Kalvas, H. Koivisto, J. Komppula, P. Peura, O. Tarvainen, and V. Toivanen, "Plasma instability in the afterglow of electron cyclotron resonance discharge sustained in a mirror trap," Phys. Plasmas **19**, 122501 (2012).
[38]I. Izotov, O. Tarvainen, V. Skalyga, D. Mansfeld, T. Kalvas, H. Koivisto, and R. Kronholm, "Measurement of the energy distribution of electrons escaping minimum-B ECR," Plasma Sources Sci. Technol. **27**, 025012 (2018).
[39]B. Isherwood and G. Machicoane, "Measurement of the energy distribution of electrons escaping confinement from an electron cyclotron resonance ion source," Rev. Sci. Instrum. **91**, 025104 (2020).
[40]B. S. Bhaskar, H. Koivisto, O. Tarvainen, T. Thuillier, V. Toivanen, T. Kalvas, I. Izotov, V. Skalyga, R. Kronholm, and M. Marttinen, "Correlation of bremsstrahlung and energy distribution of escaping electrons to study the dynamics of magnetically confined plasma," Plasma Phys. Controlled Fusion **63**, 095010 (2021).
[41]I. Izotov, O. Tarvainen, V. Skalyga, D. Mansfeld, H. Koivisto, R. Kronholm, V. Toivanen, and V. Mironov, "Measurements of the energy distribution of electrons lost from the minimum B-field—The effect of instabilities and two-frequency heating," Rev. Sci. Instrum. **91**, 013502 (2020).
[42]I. V. Izotov, A. G. Shalashov, V. A. Skalyga, E. D. Gospodchikov, O. Tarvainen, V. E. Mironov, H. Koivisto, R. Kronholm, V. Toivanen, and B. Bhaskar, "The role of radio frequency scattering in high-energy electron losses from minimum-B ECR ion source," Plasma Phys. Controlled Fusion **63**, 045007 (2021).
[43]Photomultiplier tubes: Basics and applications, https://www.hamamatsu.com/resources/pdf/etd/PMT_handbook_v3aE.pdf, 2021; accessed 14 October 2021.
[44]G. F. Knoll, *Radiation Detection and Measurement* (Wiley, New York, 1983).
[45]B. Bhaskar, H. Koivisto, L. Maunoury, O. Tarvainen, T. Thuillier, and V. Toivanen, "Quasi-periodical kinetic instabilities in minimum-B confined plasma," Phys. Plasmas (2021) (submitted).
[46]J. Kantele, *Handbook of Nuclear Spectrometry* (Academic Press, London, Great Britain, 1995).
[47]T. Ropponen, O. Tarvainen, P. Jones, P. Peura, T. Kalvas, P. Suominen, H. Koivisto, and J. Ärje, "The effect of magnetic field strength on the time evolution of high energy bremsstrahlung radiation created by an electron cyclotron resonance ion source," Nucl. Instrum. Methods Phys. Res., Sect. A **600**, 525–533 (2009).
[48]A. Kitagawa, T. Fujita, M. Muramatsu, S. Biri, R. Racz, Y. Kato, K. Yano, N. Sasaki, and W. Takasugi, "Two-frequency heating technique for stable ECR plasma," in *Proceedings of 20th Workshop on ECR Ion Sources* (JACoW, Sydney, Australia, 2012), pp. 10–12; available at https://accelconf.web.cern.ch/ECRIS2012/papers/tuxo03.pdf.
[49]V. Toivanen, O. Tarvainen, J. Komppula, and H. Koivisto, "Oscillations of ECR ion source beam current along the beam transport of the JYFL K-130 cyclotron," J. Instrum. **8**, T02005 (2013).
[50]V. Skalyga, I. Izotov, T. Kalvas, H. Koivisto, J. Komppula, R. Kronholm, J. Laulainen, D. Mansfeld, and O. Tarvainen, "Suppression of cyclotron instability in electron cyclotron resonance ion sources by two-frequency heating," Phys. Plasmas **22**, 083509 (2015).

Published under an exclusive license by AIP Publishing

[51]O. Tarvainen, T. Kalvas, H. Koivisto, J. Komppula, R. Kronholm, J. Laulainen, I. Izotov, D. Mansfeld, and V. Skalyga, "Kinetic instabilities in pulsed operation mode of a 14 GHz electron cyclotron resonance ion source," Rev. Sci. Instrum. **87**, 02A701 (2016).
[52]O. Tarvainen, J. Angot, I. Izotov, V. Skalyga, H. Koivisto, T. Thuillier, T. Kalvas, V. Toivanen, R. Kronholm, and T. Lamy, "The effect of plasma instabilities on the background impurities in charge breeder ECRIS," AIP Conf. Proc. **2011**, 070006 (2018).
[53]J. Benitez, C. Lyneis, L. Phair, D. Todd, and D. Xie, "Dependence of the bremsstrahlung spectral temperature in minimum-B electron cyclotron resonance ion sources," IEEE Trans. Plasma Sci. **45**, 1746–1754 (2017).
[54]D. Hitz, A. Girard, G. Melin, S. Gammino, G. Ciavola, and L. Celona, "Results and interpretation of high frequency experiments at 28 GHz in ECR ion sources, future prospects," Rev. Sci. Instrum. **73**, 509 (2002).
[55]R. C. Vondrasek, R. H. Scott, R. C. Pardo, and D. Edgell, "Techniques for the measurement of ionization times in ECR ion sources using a fast sputter sample and fast gas valve," Rev. Sci. Instrum. **73**, 548 (2002).
[56]M. Marttinen, J. Angot, A. Annaluru, P. Jardin, T. Kalvas, H. Koivisto, S. Kosonen, R. Kronholm, L. Maunoury, O. Tarvainen, V. Toivanen, and P. Ujic, "Estimating ion confinement times from beam current transients in conventional and charge breeder ECRIS," Rev. Sci. Instrum. **91**, 013304 (2020).
[57]O. Tarvainen, T. Kalvas, H. Koivisto, J. Komppula, R. Kronholm, J. Laulainen, I. Izotov, D. Mansfeld, and V. Skalyga, "Periodic beam current oscillations driven by electron cyclotron instabilities in ECRIS plasmas," in Proceedings of the 21st International Workshop on ECR Ion Sources, Nizhny Novgorod, Russia, 2014.
[58]V. Toivanen, G. Bellodi, D. Küchler, F. Wenander, and O. Tarvainen, "Effect of double frequency heating on the lead afterglow beam currents of an electron cyclotron resonance ion source," Phys. Rev. Accel. Beams **20**, 103402 (2017).
[59]O. Tarvainen, T. Ropponen, V. Toivanen, T. Kalvas, J. Ärje, and H. Koivisto, "Diagnostics of plasma decay and afterglow transient of an electron cyclotron resonance ion source," Plasma Sources Sci. Technol. **19**, 045027 (2010).
[60]J. Noland, O. Tarvainen, J. Benitez, D. Leitner, C. Lyneis, and J. Verboncoeur, "Studies of electron heating on a 6.4 GHz ECR ion source through measurement of diamagnetic current and plasma bremsstrahlung," Plasma Sources Sci. Technol. **20**, 035022 (2011).
[61]R. Kronholm, M. Sakildien, D. Neben, H. Koivisto, T. Kalvas, O. Tarvainen, J. Laulainen, and P. Jones, "The effect of microwave power on the Ar^{9+} and Ar^{13+} optical emission intensities and ion beam currents in ECRIS," AIP Conf. Proc. **2011**, 040014 (2018).
[62]J. Komppula and O. Tarvainen, "VUV diagnostics of electron impact processes in low temperature molecular hydrogen plasma," Plasma Sources Sci. Technol. **24**, 045008 (2015).
[63]R. Kronholm, T. Kalvas, H. Koivisto, J. Laulainen, M. Marttinen, M. Sakildien, and O. Tarvainen, "Spectroscopic study of ion temperature in minimum-B ECRIS plasma," Plasma Sources Sci. Technol. **28**, 075006 (2019).
[64]R. Kronholm, T. Kalvas, H. Koivisto, S. Kosonen, M. Marttinen, D. Neben, M. Sakildien, O. Tarvainen, and V. Toivanen, "ECRIS plasma spectroscopy with a high resolution spectrometer," Rev. Sci. Instrum. **91**, 013318 (2020).

Published under an exclusive license by AIP Publishing